

Hydraulic features of supercritical flow along prismatic side weirs

Caractéristiques hydrauliques de l'écoulement torrentiel dans des déversoirs latéraux prismatiques

GIUSEPPE OLIVETO, *PhD, Department of Environmental Engineering and Physics, University of Basilicata, C.da Macchia Romana, I-85100 Potenza, Italy*

VITTORIO BIGGIERO, *Professor, Department of Hydraulic and Environmental Engineering, University of Naples, Via Claudio 21, I-80125 Naples, Italy*

MAURO FIORENTINO, *Professor, Department of Environmental Engineering and Physics, University of Basilicata, C.da Macchia Romana, I-85100 Potenza, Italy*

ABSTRACT

Side weirs are key structures often located in combined sewer systems, provided the upstream flow is subcritical. At present, knowledge of the outflow process when the flow along the weir is subcritical can be considered satisfactory. The same cannot be said when, as often happens in practice, the upstream flow is subcritical while the flow along the weir is supercritical. In this paper the local flow features along prismatic side weirs in a circular channel were investigated. In particular, the condition of supercritical flow along the weir was analysed. Based on experimental work and on data available in the literature, some characteristics of both the flow that remains in the main channel and the flow that leaves it were investigated. These include: the distribution of the discharge in the main channel, the lateral outflow angle and the lateral outflow velocity. The results combine to provide a better understanding of the outflow process and are also readily applicable for design. Finally, a theoretical global approach is presented to estimate the head loss due to the flow partition.

RÉSUMÉ

Les déversoirs latéraux sont souvent utilisés dans les égouts à condition que l'écoulement en amont soit fluvial. Actuellement, la connaissance de l'écoulement dans des déversoirs latéraux lorsque celui-ci est fluvial peut être considéré comme satisfaisant. On ne peut pas dire la même chose lorsque, comme il arrive fréquemment dans la pratique, l'écoulement en amont est fluvial, alors que l'écoulement dans le déversoir latéral est torrentiel. Dans cette étude les caractéristiques locales de l'écoulement le long des déversoirs latéraux prismatiques dans un canal de section circulaire sont recherchées. On considère, en particulier, l'écoulement torrentiel. À l'aide des essais sur un modèle hydraulique et des données expérimentales disponibles dans la littérature, quelques caractéristiques du courant qui reste dans le canal principal et du courant qui en sort sont considérées. Ces caractéristiques sont: la répartition du débit le long du canal principal, l'angle et la vitesse de la sortie latérale. Les résultats obtenus permettent une meilleure connaissance du mécanisme d'écoulement et sont facilement utilisables pour le dimensionnement hydraulique des déversoirs latéraux. Finalement, une approche théorique est présentée pour la détermination de la perte de charge due à la partition de l'écoulement.

1 Introduction

In combined sewer systems suitable locations are selected where, during storms, the approach flow can be partitioned so that only a small fraction of water remains in the system and continues toward the sewage treatment station. The remainder is either discharged into a rainwater storage basin or led directly into a receiving water body.

To achieve this, two structures have been favoured in the last few decades: bottom openings and side weirs. The bottom opening is particularly suitable when the upstream flow is supercritical whereas the side weir is usually adopted with subcritical upstream flow.

Side weirs are usually constructed in circular, U-shaped or egg-shaped cross-sections. For discharges smaller than the design discharge of the treatment station no spill should occur. In the opposite case the side weir should work so that any discharge which exceeds the design discharge is spilled.

Apart from the channel shape, in the case of relatively large weir height, i.e. when the flow in the channel along the weir is subcritical, and provided that the weir is not too long, the outflow process

can be studied with sufficient accuracy by assuming that the specific energy in the main channel is constant [3], [2]. In the case in which the upstream flow is subcritical while the flow along the weir is supercritical, current knowledge of flow characteristics is poor, although this case is often encountered in practice. In particular, in the case of a rectangular channel, Gentilini [5] and Ferroglio [4] showed that for a side weir with low relative weir height the hypothesis of constant specific energy in the main channel cannot be assumed. Volkart [11], Uyumaz and Muslu [10] arrived at the same conclusion in the case of a circular prismatic channel.

The purpose of this paper was thus, using experimental and theoretical evidence, to provide a better understanding of the hydraulic features of supercritical flow along prismatic side weirs, with an extension to the case in which the weir height is very low. In particular, investigations on discharge distribution, lateral outflow angle and velocity were made. Therefore, a theoretical study was conducted to account for the experimentally observed specific energy change in the main channel due to the partition flow process.

Revision received April 21, 2000. Open for discussion till August 31, 2001.

2 Experiments

2.1 Experimental work

With reference to supercritical flow along a prismatic side weir, there are few data available on the local hydraulic characteristics of both the flow in the reach of the main channel in which the weir is framed and the flow along the weir. Thus, selected experiments were conducted, mainly focussed on measuring the local outflow angle and velocity along the weir.

The experiments were carried out in the Laboratory of the Hydraulic and Environmental Engineering Department of the University of Naples on an installation used previously by Biggiero et al. [1]. A Plexiglas pipe of internal diameter $D = 291$ mm was used. The pipe length from the inlet section to the beginning of the side weir was 10 m while the pipe length from the end of the side weir to the end of the channel was 8 m. The bottom slope of the channel was 0.1%. One side weir was used with relative length $L/D = 6$ and with relative weir height $c/D = 0.15$. The weir crest was sharp and parallel to the bed. Fig. 1 shows a scheme of the experimental setup.

The following test procedure was adopted. In the region of the side weir and after the flow was steady, the water depth in the channel and over the crest of the weir was measured using a point gauge to an accuracy of ± 1 mm. For each single test, at least 30 individual readings were made. Furthermore, along the weir crest and at a different distance from the beginning of the side weir numerous sections were previously selected, each of which will be, hereafter, referred to as "weir crest section". Vertically above the weir crest the local superficial outflow angle ϕ_s (with index $s = \text{surface}$) was measured. This was done by using a rodamine dye to visualise the surface flow patterns which were measured using a point gauge movable in longitudinal, transversal and vertical directions. The use of dye injection also revealed that, along the vertical direction, the outflow angle ϕ did not show

any appreciable variation, with particular regard to the sections far from the beginning of the weir. On the basis of this observation the local outflow velocity u was measured to $\pm 5\%$ accuracy at several points along the weir crest with a Pitot-Prandtl tube kept in the surface outflow streamline direction visualised by means of the tracer injected. The Pitot-Prandtl probe was designed for use in the non-hydrostatic pressure field, and its pipe, dedicated to measure the sum of the pressure and velocity head, had an external diameter of 3 mm. The two pipes of the probe were connected to a manometer. Above the weir crest, thanks to the very small streamline vertical curvature, the dynamic effects on the static openings of the Pitot-Prandtl tube were practically absent. The discharge that remained in the main channel was measured to $\pm 1\%$ by a 90° contracted V-notch weir while the overflow discharge was measured with a Venturi Flume to $\pm 2\%$. In all the experiments the upstream flow was subcritical and the flow along the weir was supercritical. The water depth crossed the critical depth before the beginning of the weir. In this section the flow depth was always very close to 0.9 times the critical depth. The water surface profile curvature was appreciable just upstream of the weir and for a short part at the beginning of the weir. Despite some curvature of the water surface, preliminary observations revealed that the pressure in the channel was approximately hydrostatic, in accordance with other previous experimental studies [1]. The flow downstream of the weir was not controlled and in all the experiments, owing to the approach flow characteristics and the weir geometry, the hydraulic jump occurred far enough from the weir. The experimental setup was such that no helical flow was observed in the channel adjacent to the weir.

2.2 Data from other sources

Besides the data collected by the authors which mainly provided an understanding of the local features of the flow that leaves the

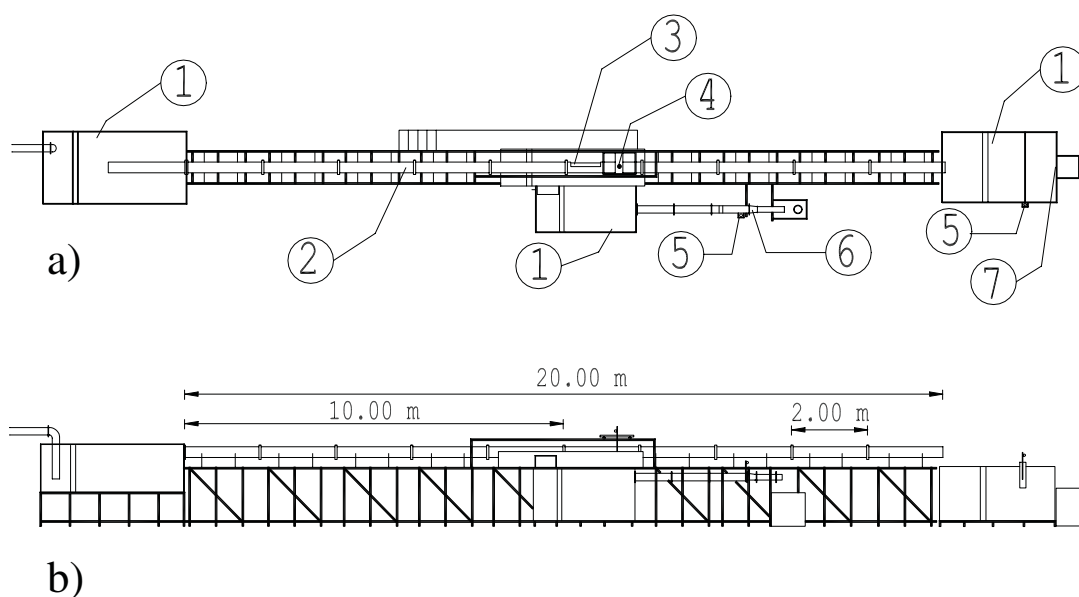


Fig. 1. Experimental arrangement: *a)* plan; *b)* side view. ① tank; ② approach pipe; ③ side weir; ④ point gauge; ⑤ piezometer; ⑥ Venturi flume; ⑦ V-notch weir.

main channel, other data, available from previous investigations referring to side weir flow in a circular, prismatic channel, were also used in this analysis. We chiefly considered the studies conducted by Sassoli [9] and Biggiero et al. [1].

The bottom slope of Sassoli's channel was 0.1% and the pipe diameter was 200 mm. The relative weir lengths were $L/D = 3, 4, 5,$ and $6,$ and the relative weir heights c/D ranging between 0.25 and 0.66 were considered. Axial flow depths were observed at intervals of $\Delta x = 200$ mm along the weir, and additional upstream and tailwater sections. The weir crest was also sharp.

The channel used by Biggiero et al. [1] was the same as that used by the authors. The relative weir lengths were $L/D = 1/3, 1, 3,$ and 6 and the relative weir heights $c/D = 0.10, 0.15, 0.25,$ and $0.35.$ The observations included the free surface profile along the weir and additional measurements in some upstream and tailwater sections. For selected runs, the longitudinal velocity component and pressure were also determined in several transverse sections along the weir. Flow depths were measured with a point gauge to the nearest mm, velocities and pressures were measured with a Pitot-Prandtl tube.

3 Experimental results

Fig. 2 shows a typical free surface that occurs along the side weir with a low relative weir height when the upstream flow is subcritical and when there are no submergence effects from the downstream pipe. In particular, longitudinally the flow depth drops quickly in a short reach close to the beginning of the weir; further downstream, the free surface becomes flatter. Transversally, the free surface shows a marked slope only in the sections close to the beginning of the weir; further downstream, this slope becomes negligible and assumes also reverse values.

3.1 Discharge distribution

The experimental data of Biggiero et al. [1] have been used to predict the discharge distribution in the reach of the main channel in which the weir is framed. To this end, 9 runs were carried out

in which the relative weir length L/D was always equal to 3, the relative weir heights c/D were 0.10, 0.15, and 0.25, and the approach discharges Q_1 were 35, 45, and 52 l/s (hereafter, subscript 1 refers to the section that we will call the "approach section", located upstream of the weir, where the flow is critical; subscript 2, refers to the section that we will call the "downstream section", located at the end of the weir).

For each run, along the weir, 5 cross-sections were considered; the first located at the beginning of the side weir, the last at the end. In each cross-section there were at least 20 measurement points of both the longitudinal velocity component and the pressure. At each cross-section the discharge was calculated by dividing the cross-section into subsections, with the centroid coinciding with a measurement point, and summing the products of the subsection area and the longitudinal velocity component at this centroid.

Fig. 3 shows the results for the case $Q_1 = 45$ l/s. It can be seen that, in the main channel, the discharge Q shows a quadratic variation with respect to the dimensionless longitudinal coordinate $X = x/D,$ and thus the outflow intensity $q = dQ/dX$ varies linearly with $X.$ Using regression analysis, the following expression was obtained:

$$\frac{Q}{Q_1} = \alpha X^2 + \beta X + 1 \quad (1)$$

in which coefficients α and β depend on the relative weir height $C = c/D$ and the relative critical depth $K = h_1/D,$ where

$$\alpha = -0.047K - 0.33C + 0.13 \quad (2)$$

$$\beta = 0.00091K + 1.68C - 0.61 \quad (3)$$

Differentiating Eq. (1) with respect to X we obtain

$$\frac{1}{Q_1} \frac{dQ}{dX} = 2\alpha X + \beta \quad (4)$$

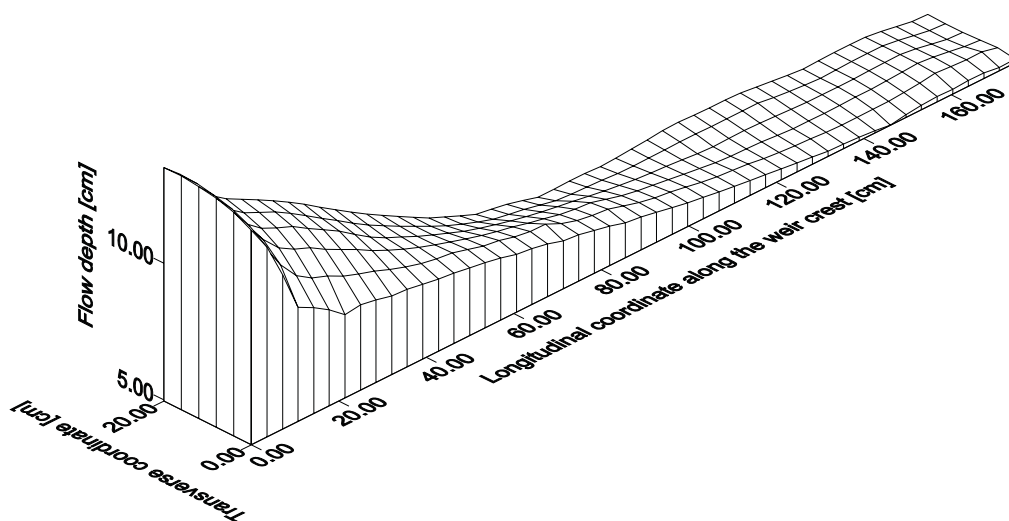


Fig. 2. Free surface along the weir for $L/D = 6, c/D = 0.15,$ and $Q_1 = 32.5$ l/s, with $Q_1 =$ approach discharge. Both the longitudinal and transverse coordinates start from the beginning of the weir crest.

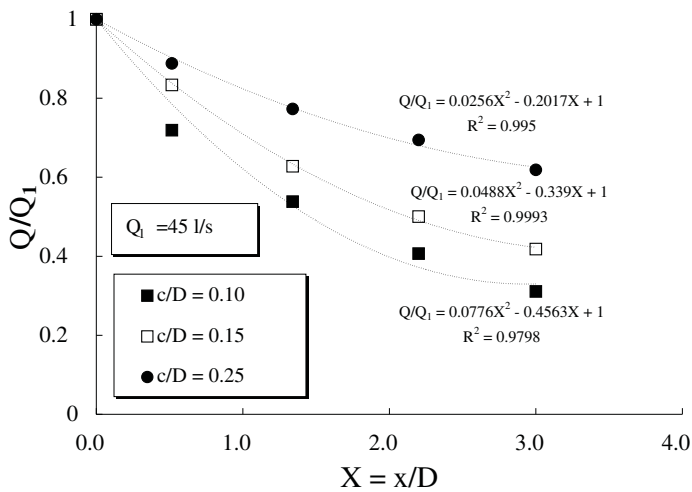


Fig. 3. Discharge ratio Q/Q_1 as a function of the dimensionless longitudinal coordinate $X = x/D$ for $Q_1 = 45$ l/s, $L/D = 3$, and $c/D = 0.10, 0.15$, and 0.25 .

Eq. (4) gives $q = 0$ when $X = -\beta/2\alpha$. Thus, inserting this value of X in Eq. (1) yields

$$\frac{Q_2}{Q_1} = \frac{\beta^2}{4\alpha} - \frac{\beta^2}{2\alpha} + 1 \quad (5)$$

or

$$\frac{Q_1 - Q_2}{Q_1} = \frac{\beta^2}{4\alpha} \quad (6)$$

where Q_2 is the discharge that remains in the main channel and, consequently, $Q_{out} = Q_1 - Q_2$ is the discharge that leaves it. The above equations are consistent when $L/D > -\beta/2\alpha$.

We noted that for $L/D = 3$ the values of Q_{out} from Eq. (6) compare well with the experimental data, whereas for $L/D = 1$ these values are systematically higher (+10%) and for $L/D = 6$ they are systematically lower (-10%). This must be attributed to a dependence of the outflow process on the relative weir length. Eq. (1) was found for the side weir with relative length $L/D = 3$. The fact that a quadratic equation well interprets the variation in discharge along the side weir is probably related to the length of the latter. If the side weir were very short, a linear function would probably be sufficiently accurate. If a longer side weir had been used, then it might have been necessary to go to a higher order polynomial. Thus, multiplying Eq. (6) by a factor that takes into account the relative weir length $\lambda = L/D$, the error can be reduced. In fact, by modifying Eq. (6) as follows

$$\frac{Q_1 - Q_2}{Q_1} = \frac{\beta^2}{4\alpha} \left(0.9 + \frac{1}{30} \lambda \right) \quad (7)$$

the deviation of calculated values of Q_{out} from experimental data is less than $\pm 5\%$ (Fig. 4).

The great advantage of Eq. (7), in predicting the outflow discharge, is that it contains only terms which depend on the weir geometry and on the approach discharge. There is no dependence

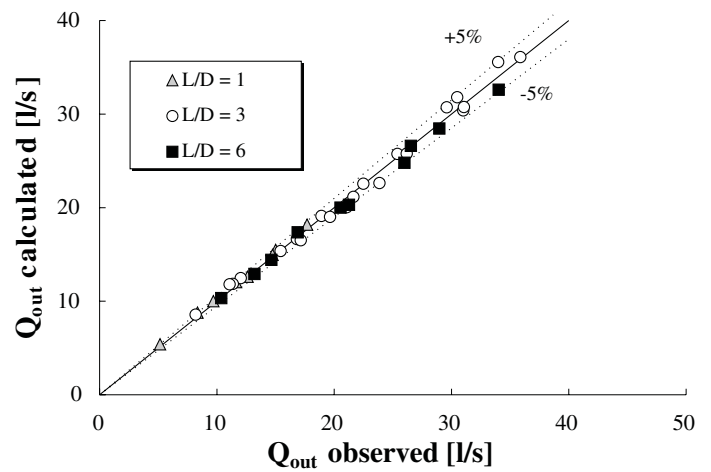


Fig. 4. Comparison between the calculated values of $Q_{out} = Q_1 - Q_2$, using Eq. (6), and the experimental data.

on the so-called discharge coefficient. In this light we did not investigate in this work the contraction effects at the weir. However, a limited number of experiments, which we conducted to this end, seems to indicate that the discharge coefficient tends to increase downstream along the weir. At the beginning of the weir a small portion of the outflow comes from the part of the flow close to the channel bed and creates an appreciable flow contraction at the weir crest; this effect tends to decrease downstream and the discharge coefficient to increase consequently.

The equations above give a simple method for the design of a side weir with a low relative weir height. In fact, for a fixed relative weir height c/D , on the basis of the uniform flow depth of the dry weather flow, one can determine (with an accuracy of $\pm 10\%$) the relative weir length required using $L/D = -\beta/2\alpha$. Then, with reference to the maximum approach discharge and by means of Eq. (7), the outflow discharge can be calculated (with an accuracy of $\pm 5\%$). Therefore, Eq. (1) can be used, with good accuracy if L/D is equal to 3, to evaluate the local outflow discharge.

4 Theoretical results

4.1 Lateral outflow velocity

In this section we will derive, based on approximations, some useful theoretical expressions for the velocity components of the flow leaving the channel. In particular, we will deal with the velocity U in the direction of the flow and its component W in the direction perpendicular to the weir crest.

As regards U , a useful expression can easily be derived, with reference to the streamline taken at the flow surface passing through points O_1 and O_2 (see Fig. 5a), by the use of Bernoulli's equation. Hence, neglecting the channel slope, the following is obtained:

$$U = \sqrt{2g(H_1 - h_w)} \quad (8)$$

where H_1 is the average specific energy at the approach section and h_w is the outflow depth measured at O_2 with respect to the channel bed (see Fig. 5b). If instead of a superficial streamline a generic path of the flow leaving the channel is considered, Eq. (8)

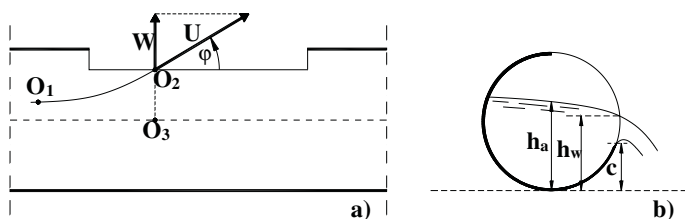


Fig. 5. Definition sketch for the lateral outflow over a side weir: a) plan view; b) transverse section.

can still be used by taking into account a number of approximations. In particular, due to the non-uniform specific energy distribution throughout the approach section, H_1 might not be completely representative of that part of the flow leaving the channel. However, in the case of low weirs, where a large part of the total approach flow is diverted, H_1 can confidently be taken as a good approximation with regard to any streamline. Moreover, along the weir crest, the pressure head is equal to zero at both the upper and lower wedges of the nappe and is slightly positive in the middle. As regards the piezometric head, this is equal to h_w on the surface and not significantly different from h_w in the middle, where the pressure head tends to counterbalance the reduction in the geometric elevation. The maximum difference between the piezometric head and h_w is found at the lower wedge, where the pressure head is equal to zero and the piezometric head equals the weir height. However, thanks to the usual small values of the difference ($h_w - c$) we can suppose that this error may be neglected.

As regards W , Bernoulli's equation can be invoked to relate points O_2 and O_3 . It leads to

$$W = \sqrt{2g(h_a - h_w)} \quad (9)$$

where h_a is the flow depth at O_3 . Eq. (9) arises from the hypothesis that the velocity component perpendicular to the main channel is mainly controlled by the piezometric head of the longitudinal flow along the channel. On the basis of experiments, we noted that a practically longitudinal flow occurs at a relatively short distance from the weir and that, with reference to the flow in the channel, the velocity component orthogonal to the weir is already negligible around the central axis of the channel. Hence, it may be assumed that at O_3 the flow velocity in the direction $O_3 - O_2$ can be neglected so that Eq. (9) can be readily derived. In order to generalise Eq. (9) for any outflow section the same approximations as discussed above with reference to h_w have to be taken into account.

On the basis of Eqs. (8) and (9) we obtain

$$\sin\varphi = \frac{W}{U} = \sqrt{\frac{h_a - h_w}{H_1 - h_w}} \quad (10)$$

where φ is the average outflow angle at the weir crest section computed, from the weir crest, in a counterclockwise direction (Fig. 5a). Consequently, the following expression is also obtained:

$$U \cos\varphi = \sqrt{2g(H_1 - h_w)} \sqrt{\frac{H_1 - h_a}{H_1 - h_w}} = \sqrt{2g(H_1 - h_a)} \quad (11)$$

in which $U \cos\varphi$ represents the longitudinal component of the outflow velocity U .

Due to the underlying assumptions, Eqs. (8) and (9) are not very accurate at the most upstream part of the weir, but their overall goodness is demonstrated by comparison of experimental values of U and $U \cos\varphi$ with the respective theoretical values. In fact, with reference to our experiments in which $L/D = 6$, $c/D = 0.15$ and the approach discharge Q_1 was 38, 32, and 26 l/s, respectively, Figs. 6a and b confirm a satisfactory agreement between the distribution, along the side weir, of the experimental values of U and $U \cos\varphi$ and their theoretical values from Eqs. (8) and (11). U is shown to increase as x/D increases; at first quickly and then more slowly. The experimental values of U and $U \cos\varphi$ reported in the figures were calculated on the basis of the measured values of the time-averaged point velocities u at different depths, selected in any weir crest section by homogeneous partition of the flow depth ($h_w - c$). At the same section the local superficial angle φ_s was measured and this value was assumed as representative of the outflow angle throughout the vertical. This last assumption was not completely accurate only in the most upstream part of the weir and sufficiently good elsewhere. Thus, in any section the velocity U was estimated as the average of the local measured u values.

4.2 Specific energy loss

The momentum equation can be used to predict the energy loss due to the flow diversion. Below we will use a procedure analogous to that developed by Oliveto et al. [8] in the analysis of spatially varied flow in the presence of bottom openings. In particular, the momentum equation will be applied between the approach section 1 and the downstream section 2. Moreover, the following assumptions will be made:

- (i) the momentum correction coefficient is equal to unity;
- (ii) the pressure distribution is hydrostatic.

Based on a large number of experiments on the same flume and under similar flow conditions, Biggiero et al. [1] showed that assumptions (i) and (ii) are confidently consistent. As regards assumption (i), they showed that at the beginning and end of the weir the pressure distribution feebly differs from the hydrostatic pressure distribution. The pressures are slightly lower than the hydrostatic pressures at the beginning of the weir and slightly greater at the end of the weir. As regards assumption (ii), the above authors showed that the momentum coefficients at sections 1 and 2 are very close to unity with less than 1% deviations. Based on our experimental data, we obtained analogous results for the momentum coefficient of the diverted flow. Moreover, in order to predict the energy loss due to the flow diversion, we will not take into account the friction losses. They are partially compensated for by the bed slope and if they were to play a significant role, they could be added to the losses due to the diversion [7]. However, the experimental data we will show later in this

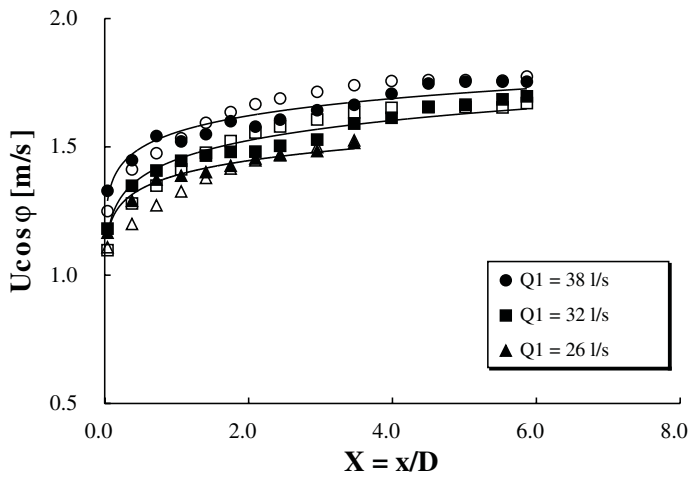
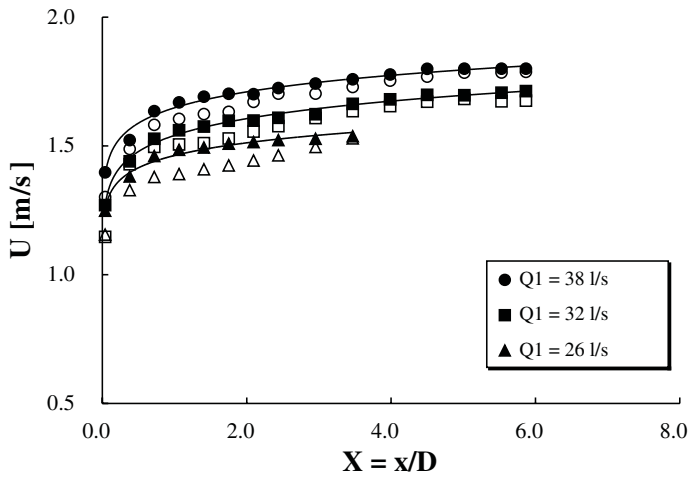


Fig. 6. Comparison between a) the average outflow velocity U calculated using Eq. (8) (solid signs) and U values obtained from experiments (open signs); b) the local longitudinal component $U \cos \varphi$ of the outflow velocity U calculated using Eq. (11) (solid signs) and the values of $U \cos \varphi$ obtained from experiments (open signs). Full curves correspond to the interpolated experimental data.

paper support the hypothesis that the friction losses can be neglected.

First we will analyse the case of a side weir in rectangular channels, then the case of a side weir in circular channels.

4.2.1 Side weir in rectangular channels

On the basis of the above assumptions, the momentum equation can be written as (see Fig. 7):

$$\frac{1}{2} \gamma h_1^2 b + \gamma \frac{Q_1^2}{g b h_1} = \frac{1}{2} \gamma h_2^2 b + \gamma \frac{Q_2^2}{g b h_2} + \gamma \frac{(Q_1 - Q_2) \bar{U} \cos \bar{\varphi}}{g} \quad (12)$$

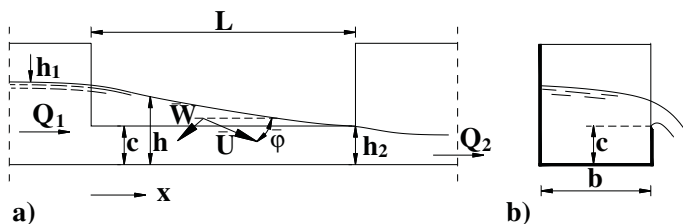


Fig. 7. Definition of parameters in a rectangular channel with a side weir: a) side view; b) transverse section.

where γ = specific weight, h = flow depth, b = channel width, Q = discharge, g = gravitational acceleration, \bar{U} = average outflow velocity along the weir, and $\bar{\varphi}$ = average outflow angle along the weir.

If $F_1 = Q_1 / (g b^2 h_1^3)^{1/2}$ is the approach Froude number, $Y = h_2 / h_1$, and $R = Q_2 / Q_1$, then Eq. (12) may be written as

$$1 + 2F_1^2 = Y^2 + \frac{2R^2 F_1^2}{Y} + \frac{2(Q_1 - Q_2) \bar{U} \cos \bar{\varphi}}{g b h_1^2} \quad (13)$$

We suppose that good estimates of \bar{U} and \bar{W} can be achieved from Eqs. (8) and (9) by simply substituting U , W , h_w and h_a with their respective average values. Hence

$$\bar{U} = \sqrt{2g(H_1 - \bar{h}_w)} \quad (14)$$

$$\bar{W} = \sqrt{2g(\bar{h}_a - \bar{h}_w)} \quad (15)$$

where, with reference to the entire weir, \bar{h}_w , \bar{h}_a and \bar{W} are the averages, along the weir, of h_w , h_a , and W respectively. In fact, although Eqs. (8) and (9) are non-linear, three experimental tests, which we conducted with reference to a side weir in circular channels, confirmed that the differences between \bar{U} and \bar{W} values calculated by Eqs. (14) and (15) and their respective experimental estimates, were always smaller than $\pm 5\%$.

Using $\sin \bar{\varphi} = \frac{\bar{W}}{\bar{U}}$, from Eqs. (14) and (15), we obtain

$$\sin \bar{\varphi} = \sqrt{\frac{\bar{h}_a - \bar{h}_w}{H_1 - \bar{h}_w}}$$

and consequently

$$\cos^2 \bar{\varphi} = 1 - \sin^2 \bar{\varphi} = 1 - \frac{\bar{h}_a - \bar{h}_w}{H_1 - \bar{h}_w} = \frac{H_1 - \bar{h}_a}{H_1 - \bar{h}_w} \quad (16)$$

Hence

$$\bar{U} \cos \bar{\varphi} = \sqrt{2g(H_1 - \bar{h}_w)} \sqrt{\frac{H_1 - \bar{h}_a}{H_1 - \bar{h}_w}} = \sqrt{2g(H_1 - \bar{h}_a)} \quad (17)$$

In particular, \bar{h}_a can be approximated by $(h_1 + h_2)/2$. Thus, Eq. (17) becomes

$$\begin{aligned} \bar{U} \cos \bar{\varphi} &= \sqrt{2g \left(H_1 - \frac{h_1 + h_2}{2} \right)} = \sqrt{2g \left[\frac{3}{2} h_1 - \frac{(1+Y)}{2} h_1 \right]} \\ &= \sqrt{g h_1 (2-Y)} \end{aligned} \quad (18)$$

Using Eq. (18) and, since in our case $F_1 = 1$, Eq. (13) becomes

$$Y^2 + 2R^2 Y^{-1} + 2(1-R)\sqrt{2-Y} - 3 = 0 \quad (19)$$

Eq. (19) gives the theoretical relation between the downstream depth Y and the discharge ratio R .

For $R = 1$ and $R = 0$ the trivial solutions are $Y = 1$ and $Y = 0$, respectively.

By assuming that at the approach and downstream sections the velocity distributions are uniform, in addition to the assumption of hydrostatic pressure distribution, the specific energy ratio $H_r = H_2/H_1$ can be written as:

$$H_r = \frac{H_2}{H_1} = \frac{h_2 + \frac{Q_2^2}{2gb^2h_2^2}}{\frac{3}{2}h_1} = \frac{h_2 + \frac{R^2Q_1^2}{2gb^2Y^2h_1^2}}{\frac{3}{2}h_1} = \frac{2}{3}Y \left(1 + \frac{R^2}{2Y^3} \right) \quad (20)$$

Eq. (20) can be rearranged to yield

$$H_r = \frac{1}{3}Y^{-2}(2Y^3 + R^2) \quad (21)$$

In this way, by using Eqs. (19) and (21) we obtain the theoretical relation between H_r and R . According to these equations, the specific energy ratio H_r is always smaller than 1; in particular, for $0 < R < 0.6$ the relative specific energy loss $(H_1 - H_2)/H_1$ is more than 10%.

Fig. 8 shows the theoretical curve $H_r = H_r(R)$ and the experimental data reported by Gentilini [5] and Ferroglio [4]. The theoretical curve is somewhat higher than the experimental results, which must be attributed to the assumptions adopted, principally, as indicated by a sensitivity analysis, to the fact that in Eq. (14) one should consider the average specific energy referred to the streamlines that leave the main channel and not to the entire cross-section.

4.2.2 Side weir in circular channels

The analytical expressions for the cross-sectional area A , the hydrostatic pressure force P , and the Froude number F of a free sur-

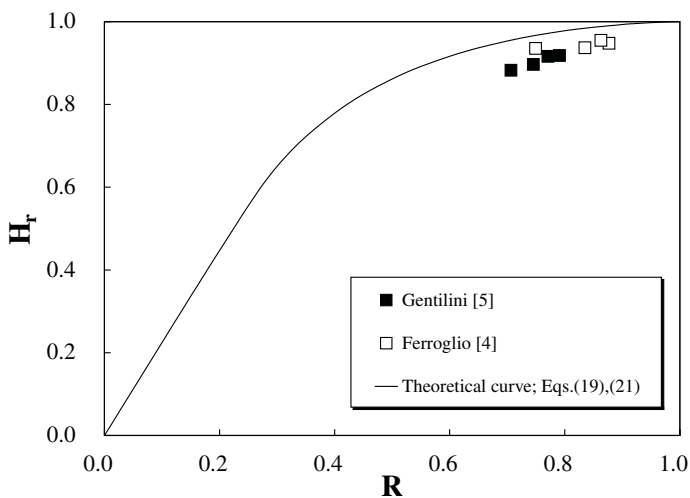


Fig. 8. Specific energy ratio $H_r = H_2/H_1$ as a function of the discharge ratio $R = Q_2/Q_1$; comparison between the theoretical curve using Eqs. (19) and (21) and the values of H_r obtained from the experimental data of Gentilini [5] (solid squares) and the experimental data of Ferroglio [4] (open squares).

face flow in a circular pipe are rather complicated. However, Hager [6] has introduced, for these variables, the following simplified expressions ($\pm 10\%$):

$$A = (Dh^3)^{1/2} \quad (22)$$

$$\frac{P}{\gamma} = \frac{1}{2}(Dh^5)^{1/2} \quad (23)$$

$$F = \frac{Q}{(gDh^4)^{1/2}} \quad (24)$$

Thus, adopting an approach analogous to that used above, the momentum equation, applied between the approach and downstream section, reads (see Fig. 9)

$$\frac{1}{2}\gamma(Dh_1^5)^{1/2} + \frac{\gamma Q_1^2}{g(Dh_1^3)^{1/2}} = \frac{1}{2}\gamma(Dh_2^5)^{1/2} + \frac{\gamma Q_2^2}{g(Dh_2^3)^{1/2}} + \frac{\gamma(Q_1 - Q_2)\bar{U} \cos \bar{\varphi}}{g} \quad (25)$$

where the symbols are the same as those used above in the case of a side weir in rectangular channels, and D is the diameter of the circular pipe.

Dividing Eq. (25) by its first term on the left-hand side and introducing the downstream depth ratio Y and the discharge ratio R , we obtain

$$1 + 2F_1^2 = Y^{3/2} + 2F_1^2Y^{-3/2}R^2 + \frac{2\bar{U} \cos \bar{\varphi}(Q_1 - Q_2)}{g(Dh_1^5)^{1/2}} \quad (26)$$

Therefore, based on Bernoulli's equation, the average outflow component in the streamwise direction $\bar{U} \cos \bar{\varphi}$ can be expressed as:

$$\bar{U} \cos \bar{\varphi} = \sqrt{2g \left(H_1 - \frac{h_1 + h_2}{2} \right)} = \sqrt{g(2H_1 - h_1 - h_2)} = \sqrt{gh_1 \left(2\frac{H_1}{h_1} - 1 - Y \right)} \quad (27)$$

so that, since $F_1 = 1$, equation (25) becomes

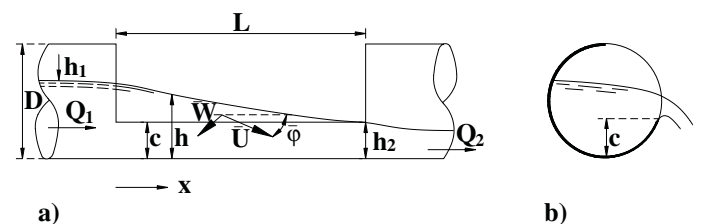


Fig. 9. Definition of parameters in a circular channel with a side weir: a) side view; b) transverse section.

$$Y^{5/2} + 2R^2Y^{-3/2} + 2\sqrt{2-Y}(1-R) - 3 = 0 \quad (28)$$

For $R = 0$ and $R = 1$ the trivial solutions are $Y = 0$ and $Y = 1$, respectively. The downstream depth is always smaller than 1 and decreases when R decreases.

Fig. 10 shows a plot $Y = Y(R)$ from Eq. (28) and the agreement with Sassoli's [9] and Biggiero et al.'s [1] experimental data may be noted.

Assuming a uniform velocity distribution at the approach and downstream section, in addition to the assumption of hydrostatic pressure distribution, the specific energy ratio can be written as

$$H_r = \frac{H_2}{H_1} = \frac{h_2 + \frac{Q_2^2}{2gA_2^2}}{h_1 + \frac{Q_1^2}{2gA_1^2}} \quad (29)$$

In this case, since in Eq. (29) the variable A is raised to 2nd power, the errors resulting from the use of the simplified expression (22) are not negligible, particularly when, as often happens at the downstream section, the filling ratio h/D is low. In any case, in order to express H_r as a function of dimensionless parameters only, with $A_r = A_2/A_1$ indicating the cross-sectional area ratio and with ζ_1 the dimensionless parameter $Q_1^2/(2gh_1A_1^2)$, Eq. (29) becomes

$$H_r = \frac{h_2}{h_1} \frac{1 + \frac{Q_2^2}{2gA_2^2h_2}}{1 + \frac{Q_1^2}{2gA_1^2h_1}} = Y \frac{1 + \zeta_1 \frac{R^2}{YA_r^2}}{1 + \zeta_1} \quad (30)$$

Thus, given the pipe diameter D and a fixed approach filling ratio h_1/D , by using Eqs. (28) and (30) the theoretical relation $H_r = H_r(R)$ may be derived.

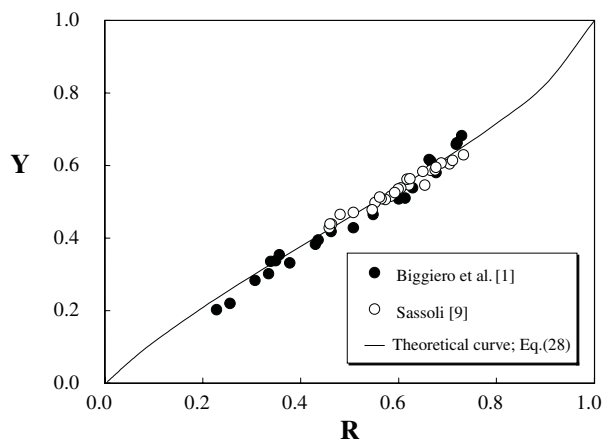


Fig. 10. Downstream depth ratio $Y = h_2/h_1$ as a function of the discharge ratio $R = Q_2/Q_1$: comparison between the theoretical curve using Eq. (28) and the experimental data of Sassoli [9] (open circles) and the experimental data of Biggiero et al. [1] (solid circles).

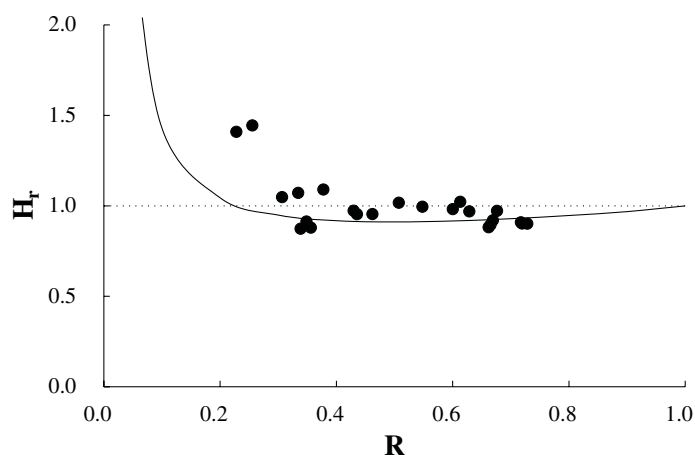
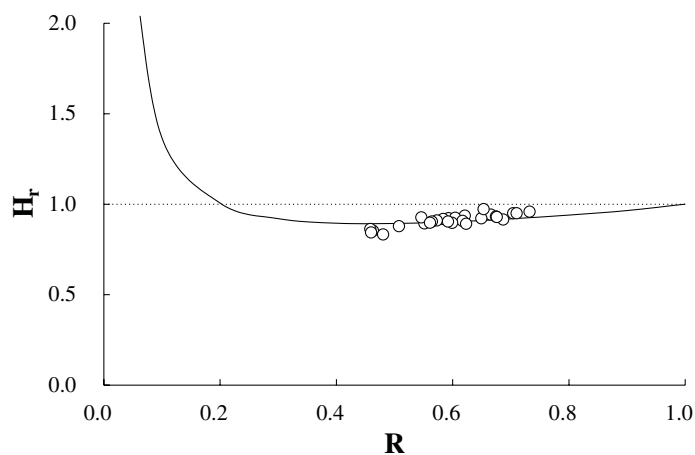


Fig. 11. Specific energy ratio $H_r = H_2/H_1$ as a function of the discharge ratio $R = Q_2/Q_1$: a) comparison between the theoretical curve using Eqs. (28) and (30) and the experimental data of Sassoli [9] (open circles); b) comparison between the theoretical curve using Eqs. (28) and (30) and the experimental data of Biggiero et al. [1] (solid circles).

Figs. 11 a and b show the function $H_r = H_r(R)$ in the case of a pipe diameter equal to that used by Sassoli [9] and Biggiero et al. [1], respectively. Therefore, the approach filling ratio h_1/D has been taken to be equal to the mean of the values h_1/D relative to the experiments made by the above authors.

4.2.3 Discussion

The results obtained show that in both circular and rectangular channels the above theoretical approach accounts for the experimental observations of specific energy variations related to the flow over side weirs (Figs. 8 and 11 a and b). According to the derived equations, the specific energy ratio H_r is not always smaller than unity. In particular, for small values of R , unlike the case of side weirs in rectangular-shaped channels, H_r increases as R approaches zero and crosses unity at very small values of R . In other words, in the case of a low crest side weir in circular-shaped channels the theoretical approach suggests that there should be an increase in specific energy due to flow separation.

A similar phenomenon was identified in the paper by Hager and Volkart [7], where the increase in specific energy of the flow in the channel along a side weir was theoretically hypothesised for

the case in which the channel velocity V is greater than $U\cos\phi$. Analogous effects were also observed in conventional junctions where the increase in specific energy in the through-branch is associated with energy loss in the lateral [6]. Moreover, in the case of a low crest side weir in circular channels, the outflow mechanism is somehow similar to that occurring in a large bottom opening, for which an increase in the specific energy of the flow in the channel had been recognised [8].

In this paper, the theory is supported by a few experiments which enforce its reliability. However, the scarcity of experimental data in the region where an increase in specific energy was found, suggests that further experimental investigations may be carried out to provide definitive confirmation of this phenomenon and thereby stimulate the search for a more detailed theoretical justification.

However, with particular regard to the comparison between the theoretical curves $H_r - R$ for side weirs in circular and rectangular channels, the fact that for very low crest height the former definitely behaves differently from the latter can be ascribed, according to Eqs. (20) and (30), to the different rates at which, in these two cases, the downstream cross sectional area A_2 varies as Q_2 approaches zero. This effect is substantially independent of the approximation on which the theory is based.

5 Conclusions

In this paper we present the results obtained from a theoretical and experimental study conducted on the flow separation process that occurs along a side weir when the flow along the weir is supercritical while upstream flow is subcritical. The main results can be summarised as follows:

- (i) the discharge Q in the main channel shows a quadratic variation with the dimensionless longitudinal coordinate $X = x/D$. This is equivalent to saying that the outflow intensity $q = dQ/dX$ decreases linearly with x/D . Based on this statement, empirical relations, independent of the so-called discharge coefficient, have been found for the side weir design. With these relations one can determine the length of the weir and then predict the global outflow discharge with an accuracy of $\pm 5\%$;
- (ii) based on Bernoulli's equation theoretical relations have been derived for the average lateral outflow velocity along the side weir and for the component in the direction perpendicular to the weir crest. Good agreement with experimental data has been demonstrated;
- (iii) theoretical and experimental results dealing with the possible increase in the specific energy of the flow in the case of side weirs with very low crest would suggest the desirability of more detailed investigations of the outflow process in this case of a large outflow discharge.

Acknowledgements

The authors would like to thank Professor W.H.Hager from ETH-Zurich for his helpful suggestions with regard to both theoretical analysis and experimental work. Comments and suggestions by

two anonymous referees are also acknowledged and sincerely appreciated.

Notations

A	cross sectional area
b	channel width
$C = c/D$	relative weir height
c	height of weir
D	pipe diameter
F	Froude number
g	gravitational acceleration
h	flow depth
H	specific energy
$K = h_c/D$	relative critical depth
L	length of weir
P	pressure force
$q = dQ/dX$	outflow intensity
Q	discharge
$R = Q_2/Q_1$	discharge ratio
U	lateral outflow velocity
u	local outflow velocity
V	channel velocity
W	lateral outflow velocity component in the direction perpendicular to the weir crest
$X = x/D$	dimensionless longitudinal coordinate
x	longitudinal coordinate
$Y = h_2/h_1$	height ratio
α, β	coefficients
$\lambda = L/D$	relative weir length
ϕ	local outflow angle
γ	specific weight
$\zeta = Q^2/(2ghA^2)$	dimensionless parameter

Subscripts

1	approach section
2	downstream section
a	axis
out	outflow
r	ratio
s	surface
w	weir

References/Bibliographie

- BIGGIERO, V., LONGOBARDI, D., and PIANESE, D. (1994). Analisi sperimentale del comportamento idraulico degli sfioratori laterali a bassa soglia. *Giornale del Genio Civile*, Vol. 132, (3), pp. 183-199 (in Italian).
- CHOW, V.T. (1959). *Open channel hydraulics*. McGraw-Hill Inc., New York, N.Y.
- DE MARCHI, G., (1934). Saggio di teoria del funzionamento degli stramazzi laterali. *L'Energia Elettrica*, Vol. XI, (11), pp. 849-860 (in Italian).
- FERROGLIO, L. (1942). Ricerche sperimentali sugli sfioratori

- lateral. *L'Energia Elettrica*, Vol. XIX, (1), pp.11-19 (in Italian).
5. GENTILINI, B. (1938). Ricerche sperimentali sugli sfioratori longitudinali. *L'Energia Elettrica*, Vol. XV, (9), pp.583-595 (in Italian).
 6. HAGER, W.H. (1994). *Abwasserhydraulik*. Springer: Berlin, Germany (in German).
 7. HAGER, W.H. and VOLKART, P.U. (1986). Distribution channels. *Journal of Hydraulic Engineering*, ASCE, Vol. 112, (10), pp. 935-952.
 8. OLIVETO, G., BIGGIERO, V., and HAGER, W.H. (1997). Bottom outlet for sewers. *Journal of Irrigation and Drainage Engineering*, ASCE, Vol.123 (4), pp. 246-252.
 9. SASSOLI, F. (1963). Ricerca sperimentale sugli sfioratori laterali in canali a sezione circolare. Parte seconda: Andamento e tracciamento dei profili liquidi. *Atti VIII Convegno di Idraulica e Costruzioni Idrauliche*, Mem. A-12, Pisa, Italy, pp. 1-18 (in Italian).
 10. UYUMAZ, A. and MUSLU, Y. (1985). Flow over side weirs in circular channels. *Journal of Hydraulic Engineering*, ASCE, Vol. 111, (1), pp. 144-160.
 11. VOLKART, P.U. (1983). Spatially varied flow over short side weirs in channels of circular shape. *Proceedings XX IAHR Congress*, Vol. VI, Moscow, U.S.S.R., pp. 519-526.